Journal of the Korean Ceramic Society
Vol. 41, No. 7, pp. 497~502, 2004.

Hybrid Coextrusion and Lamination Process for Macrochanneled Bioceramic Scaffolds

Young-Hag Koh,† Chang-Jun Bae, and Hyoun-Ee Kim

School of Materials Science and Engineering, Seoul National University, Seoul 151-742, Korea
(Received May 29, 2004; Accepted June 8, 2004)

ABSTRACT

A hybrid coextrusion and lamination process has been developed to fabricate macrochanneled bioceramic scaffolds. This process was mainly composed of three steps (i.e., coextrusion of thermoplastic compound, lamination, and thermal treatment), forming unique pore channels in dense bioceramic body. Pore channels were formed by removing carbon black material, while calcium phosphate or Tetragonal Zirconia Polycrystals (TZP) with a calcium phosphate coating layer were used as dense body. Two kinds of pore structures were fabricated; that is, the pore channels were formed in uni- or three-directional array. Such macrochanneled bioceramic scaffolds exhibited the precisely controlled pore structure (pore size, porosity, and interconnection), offering excellent mechanical properties and cellular responses.

Key words : Bioceramics, Scaffold, Porous body, Coextrusion, Macrochannel

1. Introduction

Recently, the fabrication of bioceramics with porous configurations has attracted particular attention because a porous network allows tissue infiltration, which in turn enhances implant-tissue attachment.[1-3] However, conventional pore forming methods, such as the hydrothermal exchange process,[4] the pyrolysis of organic particles,[5-7] and polyurethane sponge techniques, 8 have shown limited control over the pore geometry. As a result, these porous HA bodies have a wide range of porosity and pore sizes with a much smaller interconnecting fenestration.

Among bioceramics, calcium phosphate has been regarded as a promising biomaterial due to its high biocompatibility, good bioaffinity and osteoconduction, and its crystallographic and chemical similarity to human bone.[9-12] When HA materials are used as implants, they are slowly replaced by the host bone, forming a direct bond with the neighboring bone structure. However, this material suffers from low mechanical properties.[13-15] On the other hand, tetragonal zirconia polycrystals (TZP-3 mol% yttria-zirconia) possesses excellent mechanical properties, such as high strength, toughness, and compressive strength.[9] In spite of these merits, its bio-inert nature have limited its wider applications.

Therefore, in this paper, we developed a novel process, named "hybrid coextrusion and lamination" to precisely control the pore geometry (i.e., aligned pore channel). This process was simply comprised of coextrusion, and lamination, and thermal treatment, offering uniform array of macrochannels on the sintered body. Calcium phosphate or Tetragonal Zirconia Polycrystals (TZP) with a calcium phosphate coating layer were used as dense body. Pore channels were formed by removing carbon black material. Such pore channels were formed in uni- or three-directional array. Various macrochanneled bioceramic scaffolds were fabricated. The sintered samples were analyzed by X-Ray Diffraction (XRD), optical microscopy, Scanning Electron Microscopy (SEM), and Electron Dispersive Spectroscopy (EDS) analysis. Also, the compressive strengths were also measured and cellular responses were evaluated.

2. Experimental Procedure

Commercially available calcium phosphate (Sigma-Aldrich Co., Milwaukee, WI) and tetragonal zirconia polycrystals (TZ-3Y; Tosoh Co., Tokyo, Japan) powder were used as the bioceramics. Carbon black powder (Cabot Black Pearls BP-120; Cabot Corp., Boston, MA) was used as a fugitive material, which could be removed after a thermal treatment, forming a macrochannel. The calcium phosphate powder was calcined at 900°C for 1 h in air in order to improve the powder characteristics. The ceramic (or fugitive) powder was mixed with an ethylene ethyl acrylate (EEA; EEA 6182; Union Carbide, Danbury, CT)-based resin at 105°C using a high shear mixer. Also, agents were added as processing aids to ensure a consistent apparent viscosity value (~3000 Pa·s).

Two different pore structures with the uni- or three-directional array of pore channel were fabricated. At first, initial

†Corresponding author : Young-Hag Koh
E-mail : kohyh@snu.ac.kr
Tel : +82-2-880-1397 Fax : +82-2-884-1413

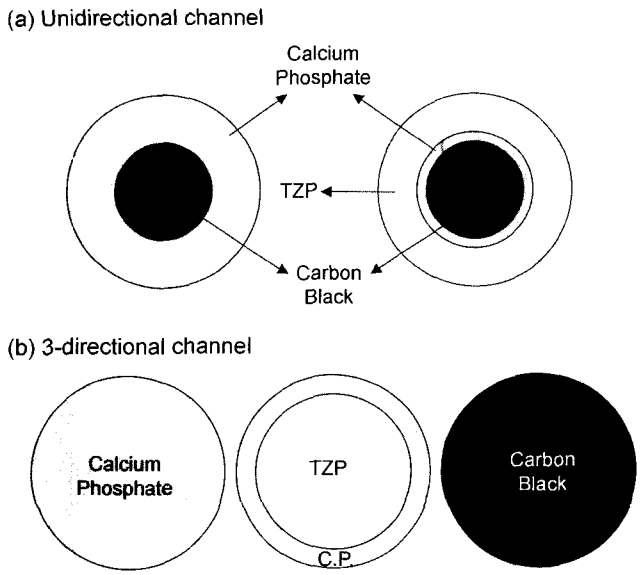

Fig. 1. Schematics illustrating the cross-sections of the initial feedrods for (a) the unidirectional macrochannel and (b) the 3-directional macrochannel.

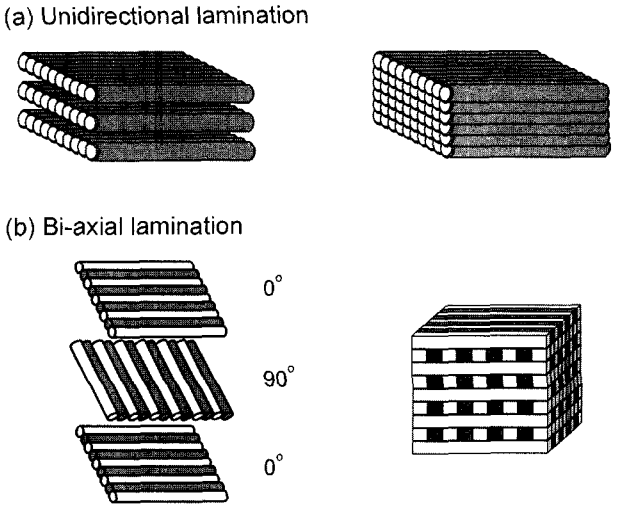

Fig. 2. Schematics illustrating (a) the unidirectional lamination and (b) the bi-axial lamination. Note, right schematics represent the laminated structures.

feed rod was prepared using either a 22-mm cylindrical mold or a half-piped mold. The schematic of initial feedrods are illustrated in Fig. 1(a) and (b) for the unidirectional and 3-directional macrochannel, respectively. For unidirectional macrochannel, an initial feedrod, which was comprised of ceramic (calcium phosphate or TZP/calcium phosphate) and fugitive layer, was coextruded through a 750-μm using a piston extruder at 120°C at a rate of 3 mm/min. This produced a continuous and flexible filament with the same cross-section as the initial feedrod. Each sheet was cut and unidirectionally stacked into a 38 × 38 mm metal mold then warm-pressed at 140°C with an applied load of 10 MPa. However, for the 3-directional macrochannel, the initial feedrod (ceramic or carbon black) was extruded through a 300-μm orifice. Two types of filaments (ceramic and carbon black) were set out alternately and warm-pressed at 140°C with am applied load of 10 MPa to produce filament sheet, in which carbon black filaments neighbored by ceramic filaments. The schematics of the unique filament alignment and lamination are illustrated in Fig. 2(a) and (b).

The macrochannels were formed by thermally removing the carbon black and binder from the green billets without disturbing the structures. The binder burnout was done in an alumina tube-furnace at a slow heating rate (3~10°C/h) up to 700°C in flowing air to avoid the formation of defects, such as bloating and crack. After binder burnout, the billets were sintered at temperatures ranging from 1350°C to 1600°C for 1 h in air. The sintered macrochanneled body was sliced into dimensions of 3 × 3 × 3 mm with a diamond saw to produce the specimens for measuring the compressive strength. All surfaces were polished down to 30 μm with a resin bonded diamond wheel. The compressive strengths were measured both normal and parallel to the macrochannel directions. Five specimens were tested for each experimental condition. In addition, the sintered body was analyzed using optical microscopy and XRD analysis.

The cellular response of the 3-directionally macrochanneled calcium phosphate scaffold was evaluated. After culturing for 4 days, the morphologies of the proliferated cells on macrochanneled HA scaffolds were observed with SEM. Also, the cell proliferation was assessed by MTT method after culturing for 4 days. The cell differentiation characteristics of the cell were evaluated by the alkaline phosphatase (ALP) activity expression level after culturing for 14 days.

3. Results

3.1. Unidirectionally Macrochanneled Scaffold

Fig. 3(a) and (b) shows cross sections of green 780-micron filaments consisting of ceramic (calcium phosphate and TZP clad with calcium phosphate layer) and carbon black. For macrochanneled TZP scaffold, a bioactive calcium phosphate layer continuously and uniformly surrounds the carbon black (Fig. 3(b)). These filaments were unidirectionally aligned without any gap, as shown in Fig. 3(c).

After sintering at 1350°C for 1 h, only crystalline hydroxyapatite (HA; $Ca_{10}(PO_4)_6(OH)_2$) phase was observed for the macrochanneled calcium phosphate scaffold with full densification, as shown in Fig. 4(a). On the other hand, the macrochanneled TZP scaffold exhibited a trace of the calcium phosphate peak with strong tetragonal ZrO_2 peaks was observed. The crystalline phase of the calcium phosphate was identified as crystalline tricalcium phosphate (TCP; $Ca_3(PO_4)_2$) instead of HA phase, as shown in Fig. 4(b). When calcium phosphate is sintered at high-temperatures, the TCP phase becomes more thermodynamically stable than crystalline hydroxyapatite phase, leaving CaO (s) phase.[9] In addition, with the presence of zirconia, CaO (s) reacts with the partially stabilized zirconia, forming a CaO-ZrO_2 solid solution.[16]

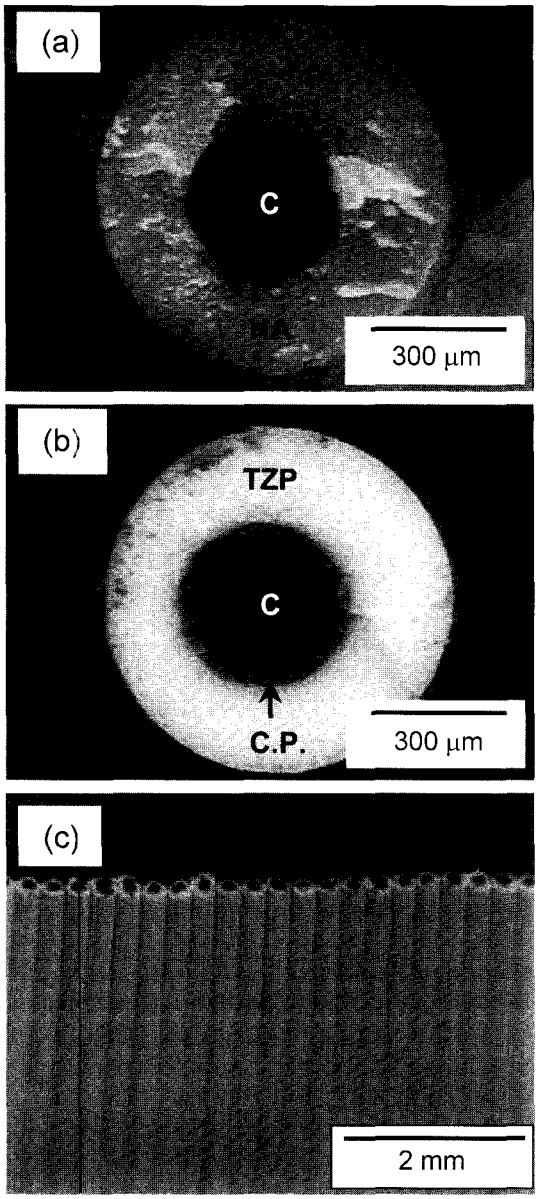

Fig. 3. Optical photographs illustrating (a) the cross-section of the calcium phosphate/carbon black filament, (b) the cross-section of the TZP/calcium phosphate/carbon black filament, and (c) the aligned filament sheet.

After sintering, the uniform array of macrochannel was formed both macrochanneled HA and TZP scaffold. A typical optical micrograph is shown in Fig. 5(a). The body consisted of 24 vol% macrochannels as a uniform array of 297-micron smooth cylinders. Furthermore, each macrochannel was clad on the inside with a 42-micron thick layer of a bioactive calcium phosphate, as shown in Fig. 5(b). No cracking

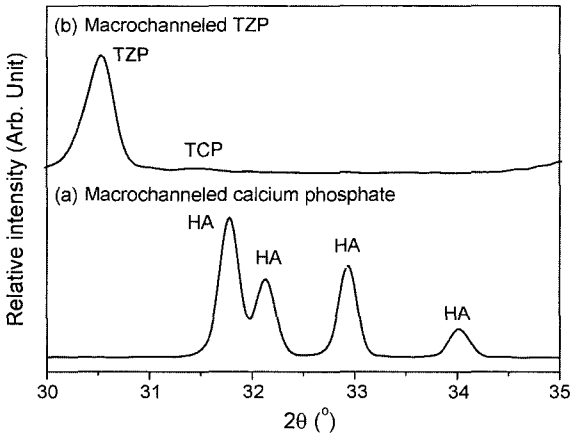

Fig. 4. XRD patterns (a) of the macrochanneled calcium phosphate and (b) of the macrochanneled TZP with a calcium phosphate coating layer sintered at 1350°C for 1 h in air.

at the TZP and calcium phosphate interfaces was observed despite the high thermal stress. Such good adhesion instead of cracking is believed to be the result of the formation of a porous calcium phosphate layer and the reaction between the ZrO_2 and Ca^{2+} ions at the interface. Similarly, 28 vol% of a 312-micron cylindrical array macrochannels was formed for the macrochannelled-calcium phosphate.

The compressive strength of the macrochanneled calcium phosphate and TZP were measured, as shown in Table 1. All samples showed the brittle fracture during compression test. As expected, the compressive strength of the macrochannelled-TZP was almost three times higher than that of the macrochanneled-calcium phosphate because of the higher mechanical properties of TZP material.

3.2. Three-Directionally Macrochanneled Scaffold

As previously mentioned, the TZP bioceramic was used for the body, which retained the applied stress, while the TZP surface was coated with calcium phosphate to ensure an active osteoconductive behavior. Also, the macrochanneled calcium phosphate scaffold was fabricated. A cross-sectional view of a filament of the TZP/calcium phosphate, made by coextrusion, is shown in Fig. 6(a). As expected, the filament shows the same design as the initial feedrod, i.e. a 16-micron calcium phosphate layer continuously and uniformly surrounded the TZP core. Furthermore, neither a gap nor overlapping was observed in the unidirectionally aligned filament sheet (Fig. 6(b)). Each sheet was bi-axially stacked to build the 3-directionally connected structure. Note, the TZP surrounded by calcium phosphate and carbon black appear in the bright and in dark contrast, respectively.

Table 1. Summary of the Properties of the Macrochanneled-TZP and Macrochanneled-Calcium Phosphate

Samples	Macrochannel fraction (vol%)	Macrochannel size (μm)	Compressive strength (MPa)
Macrochanneled TZP	24	297 ± 11	398 ± 39
Macrochanneled calcium phosphate	28	312 ± 13	132 ± 11

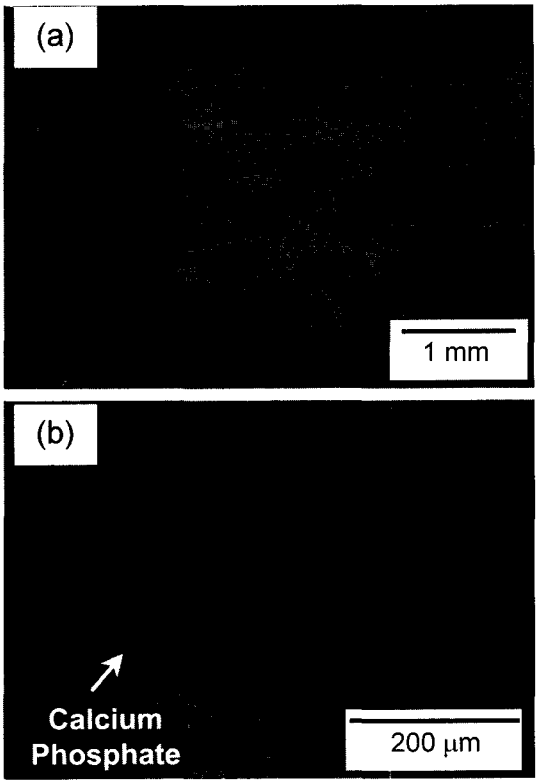

Fig. 5. Optical photographs of the macrochanneled-TZP (a) at low magnification and (b) at high magnification.

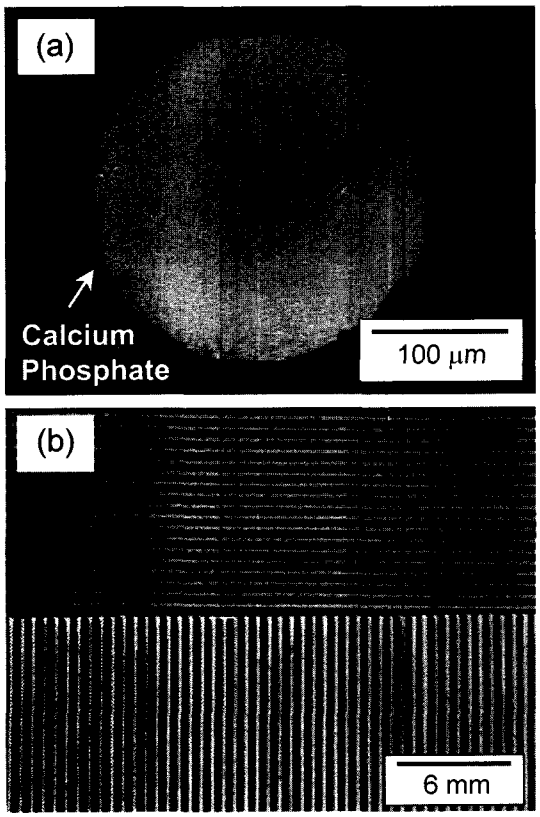

Fig. 6. Optical photograph illustrating (a) the cross-sectional view of the TZP/calcium phosphate filament and (b) the bi-axially stacked filament sheet.

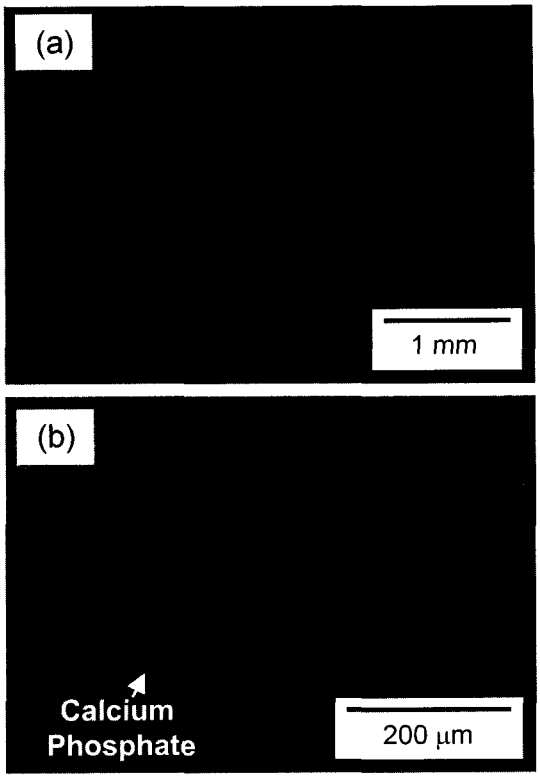

Fig. 7. Optical photographs (a) at top-view and (b) at side-view of 3-directionally macrochanneled TZP.

The optical photograph of the top-view of the sintered 3-directionally macrochannelled-TZP-coated by calcium phosphate is shown in Fig. 7(a). The body consisted of a 48 vol% TZP coated by calcium phosphate and a 52 vol% macrochannel in a uniform array of 290-microns (see Table 2). Correspondingly, 48 vol% macrochannels, 278-micron in size, were formed in the sintered calcium phosphate body.

The bioactive calcium phosphate coating layer is shown in Fig. 7(b). The interfaces between the TZP and calcium phosphate, indicated by the arrows, showed no cracking. At higher magnification, a good interfacial bonding was observed. The macrochannel was clad on the inside with a bioactive calcium phosphate layer.

As expected, the compressive strength (96 ± 11 MPa) of the 3-directionally macrochanneled-TZP was almost four times larger (24 ± 5 MPa) than that of the 3-directionally macrochanneled-HA, as described in Table 2. The remarkable improvement in compressive strength was due to the strong TZP body, which could retain a higher applied compressive stress. Furthermore, its active osteoconductive behavior is expected because its bio-inert surface is coated by a bioactive calcium phosphate layer, forming a direct bonding by being replaced by natural bone.

To investigate the cellular response of macrochanneled scaffold, the macrochanneled calcium phosphate scaffold was examined as a representative. Typical cell growth morphologies on the macrochanneled calcium phosphate scaffold after culturing 4 days are shown in Fig. 8. The HA

Table 2. Summarized Properties of the 3-Directionally Macrochanneled-TZP and 3-Directionally Macrochanneled-Calcium Phosphate

Samples	Macrochannel fraction (vol%)	Macrochannel size (μm)	Compressive strength (MPa)
3-Directionally macrochanneled TZP	52	290 ± 17	96 ± 11
3-Directionally macrochanneled calcium phosphate	48	278 ± 14	24 ± 5

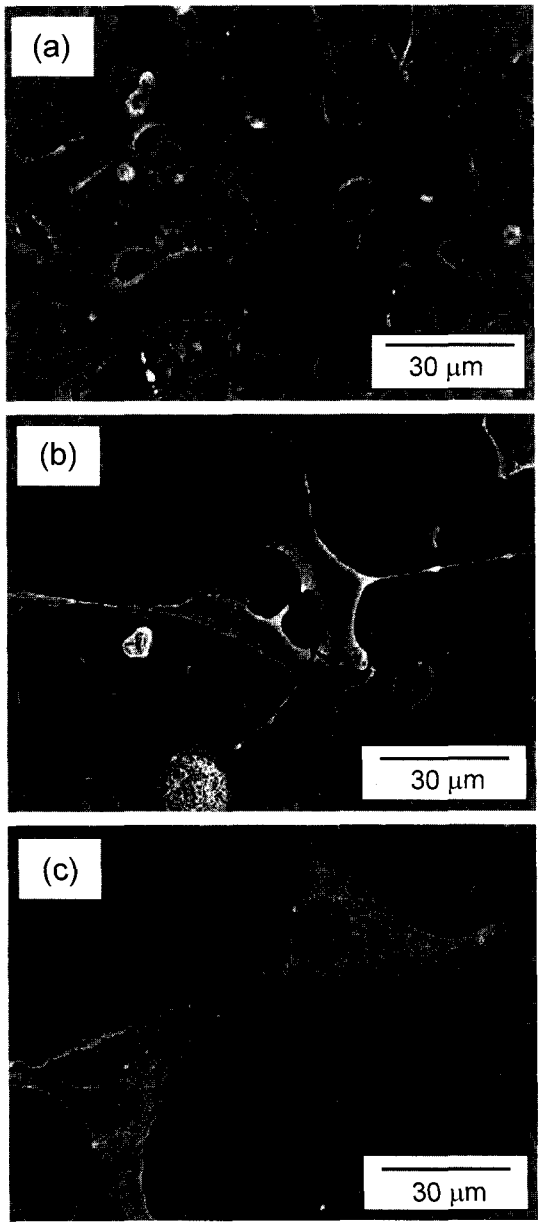

Fig. 8. SEM micrographs of HOS cells growing (a) on the top, (b) on the side, and (c) on the bottom of the macrochanneled calcium phosphate scaffold after culturing for 4 days.

framework was completely covered by the osteoblast-like cells and the cell membranes spread well with an intimate contact with the HA surface (Fig. 8(a)). Furthermore, the migration of the cells throughout the macrochannel was also observed (Fig. 8(b) and (c)), implying the osteoconducting characteristics of the macrochanneled scaffolds.

The relative number of the proliferated cells was estimated from the absorbance value. The relative absorbance value of the macrochanneled calcium phosphate scaffold was increased by a factor of 1.3 compared to that of the dense calcium phosphate. Such improvement was attributed to the increase in surface area. Similar ALP activity values were observed for the macrochanneled calcium phosphate scaffold and the dense calcium phosphate, indicating their excellent biocompatibility.

Compared to the conventional methods for manufacturing a porous body, the pore structure was precisely controlled using a hybrid coextrusion and lamination. This process is simple and effective to control the pore structure. The macrochannel is almost straight with an extremely narrow size distribution because this macrochannel is formed by removing the carbon black filament. Furthermore, the macrochannel can be formed in three-directional array, in which the interconnection size is the same as the macrochannel size, which is important for osteoconductive behavior. Another merit is that strong TZP material coated with bioactive calcium phosphate layer can be sintered without any further treatment, such as dip-coating. A preliminary observation about the cellular response of macrochanneled calcium phosphate scaffold implies that such macrochanneled bioceramic scaffolds (both calcium phosphate and TZP with calcium phosphate coating layer) are suitable as porous implants. Furthermore, it is believed that macrochanneled TZP scaffold can offer excellent biocompatibility and mechanical properties since a strong TZP body maintains its excellent mechanical properties and the calcium phosphate layer is expected to be gradually replaced by natural bone.

4. Summary and Conclusions

The macrochanneled bioceramic scaffolds were fabricated by a hybrid coextrusion and lamination process. This novel process was based on the coextrusion of thermoplastic compound (ceramic and carbon black) and unique lamination (uni or bi-axial lamination). Aligned pore channels were formed by removing carbon black material, while calcium phosphate or Tetragonal Zirconia Polycrystals (TZP) with a calcium phosphate coating layer were used as dense body. This process offered either uni- or 3-directional macrochannels on dense bioceramic. Such macrochanneled bioceramic scaffolds exhibited excellent mechanical properties and cellular responses with the precisely controlled pore structure (pore size, porosity, and interconnection).

REFERENCES

1. M. Jarcho, "Calcium Phosphate Ceramics as Hard Tissue Prosthetics," *Clin. Orthop. Relat. Res.*, **157** 259-78 (1981).
2. H. M. Rosen, "Porous, Block HA as an Interpositional Bone Graft Substitute in Orthognatic Surgery," *Plast. Reconstr. Surg.*, **83** 985-90 (1989).
3. N. Passuti, G. Daculsi, J. M. Rogez, S. Martin, and J. V. Bainvel, "Macroporous Calcium Phosphate Ceramic Performance in Human Spine Fusion," *Clin. Orthop. Relat. Res.*, **248** 169-76 (1989).
4. D. M. Roy and S. K. Linnehan, "HA Formed from Coral Skeletal Carbonate by Hydrothermal Exchange," *Nature (London)*, **247** 220-22 (1974).
5. D.-M. Liu, "Fabrication and Characterization of Porous Hydroxyapatite Granules," *Biomaterials*, **17** 1955-57 (1996).
6. M. Fabbri, G. C. Celotti, and A. Ravaglioli, "Granulates Based on Calcium Phosphate with Controlled Morphology and Porosity for Medical Applications : Physico-Chemical Parameters and Production Technique," *Biomaterials*, **15** 474-77 (1994).
7. D.-M. Liu, "Control of Pore Geometry on Influencing the Mechanical Property of Porous Hydroxyapatite," *J. Mater. Sci. Lett.*, **15** 419-21 (1996).
8. H. W. Kim, S. Y. Lee, C. J. Bae, Y. J. Noh, H. E. Kim, H. M. Kim, and J. S. Ko, "Porous ZrO_2 Bone Scaffold Coated with Hydroxyapatite with Fluorapatite Intermediate Layer," *Biomaterials*, **24** [19] 3277-84 (2003).
9. L. L. Hench, "Bioceramics: From Concept to Clinic," *J. Am. Ceram. Soc.*, **74** [7] 1487-510 (1991).
10. R. Z. Legeros, "Apatites in Biological Systems," *Prog. Cryst. Grow. Char.*, **4** 1-45 (1981).
11. C. Lavernia and J. M. Schoenung, "Calcium Phosphate Ceramics as Bone Substitutes," *Am. Ceram. Soc. Bull.*, **70** [1] 95-100 (1991).
12. T. S. B. Narasaraju and D. E. Phebe, "Review : Some Physicochemical Aspects of Hydroxyapatite," *J. Mater. Sci.*, **31** [1] 1-21 (1996).
13. D. M. Liu, "Influence of Porosity and Pore Size on the Compressive Strength of Porous Hydroxyapatite Ceramic," *Ceram. Inter.*, **23** 135-39 (1997).
14. J. C. Huec, T. Schaeverbeke, D. Clement, J. Faber, and A. Le Rebeller, "Influence of Porosity on the Mechanical Resistance of Hydroxyapatite Ceramics Under Compressive Stress," *Biomaterials*, **16** 113-18 (1995).
15. Y.-H. Koh, H.-W. Kim, H.-E. Kim, and J. W. Halloran, "Fabrication of Macrochannelled-Hydroxyapatite Bioceramic by Coextrusion Process," *J. Am. Ceram. Soc.*, **85** [10] 2578-80 (2002).
16. H.-W. Kim, Y.-H Koh, J.-Y. Noh, H.-E. Kim, and H. M. Kim, "Effect of CaF_2 on Densification and Properties of Hydroxyapatite-Zirconia Composites for Biomedical Applications," *Biomaterials*, **23** 4113-21 (2002).